

Dynamics of RNA Bacteriophage MS2 Observed with a Long-Lifetime Metal-Ligand Complex

Jung Sook Kang* and Ji Hye Yoon

Department of Oral Biochemistry and Molecular Biology, College of Dentistry, Pusan National University, Pusan 602-739, Korea

[Ru(2,2'-bipyridine)₂(4,4'-dicarboxy-2,2'-bipyridine)]²⁺ (RuBDc) is a very photostable probe that possesses favorable photophysical properties including long lifetime, high quantum yield, large Stokes' shift, and highly polarized emission. To evaluate the usefulness of this luminophore (RuBDc) for studying macromolecular dynamics, its intensity and anisotropy decays when conjugated to RNA bacteriophage MS2 were examined using frequency-domain fluorometry with a high-intensity, blue light-emitting diode (LED) as the modulated light source. The intensity decays were best fit by a sum of two exponentials, and the mean intensity decay time was 442.2 ns. The anisotropy decay data showed a single rotational correlation time (2334.9 ns), which is typical for a spherical molecule. The use of RuBDc enabled us to measure the rotational correlation time up to several microseconds. These results indicate that RuBDc can be useful for studying rotational diffusion of biological macromolecules.

key words: Long-lifetime metal-ligand complex, Macromolecular dynamics, MS2, Rotational diffusion, Light-emitting diode

INTRODUCTION

Long-lifetime metal-ligand complexes (MLCs), which display decay times ranging from 100 ns to more than 10 μ s, have only recently become available [1-3] and show a number of characteristics that make them versatile biophysical probes. Because of the large Stokes' shift, the MLCs do not display significant radiative or nonradiative homo energy transfer [2, 3]. Consequently, they do not self-quench even for a protein randomly labeled with several MLCs. In general, the MLCs display good water solubility and high thermal, chemical, and photochemical stability [2, 3]. In addition, the long lifetimes of the MLCs allow the use of gated detection, which can be employed to suppress interfering autofluorescence from biological samples and can thus provide increased sensitivity [4]. Finally, most MLCs display polarized emission, making them useful for microsecond hydrodynamics [2, 3, 5-19].

A number of Os, Re, and Ru complexes have been synthesized and used to study microsecond dynamics of proteins [5-12], lipid vesicles [6, 13-15], and DNA [16-19]. Because [Ru(bpy)₂(dcbpy)]²⁺ (bpy = 2,2'-bipyridine, dcbpy = 4,4'-dicarboxy-2,2'-bipyridine) (RuBDc) showed the largest fundamental anisotropy among the Ru complexes [8, 10], this probe is one of the most promising MLCs for studying macromolecular hydrodynamics. RuBDc has been used to monitor the rotational motions of high-molecular-weight (MW) proteins

such as concanavalin A [10], human serum albumin [8, 10], ferritin [10], immunoglobulin (Ig) G [10, 12], and IgM [12].

To evaluate further the usefulness of RuBDc for macromolecular dynamics, we measured the intensity and anisotropy decays of RuBDc conjugated to RNA bacteriophage MS2 which has a MW of 3.9×10^6 [20]. For this study, we used frequency-domain (FD) fluorometry with a high-intensity, blue light-emitting diode (LED) as the modulated light source. With this LED we were able to directly modulate the excitation light up to 100 MHz without the need for an external modulator like a Pockels cell and to obtain very reliable time-resolved intensity and anisotropy decays with simpler and low cost instrumentation.

MATERIALS AND METHODS

Materials

The *E. coli* C-3000 and phage MS2 were purchased from ATCC (Manassas, USA). The PF₆⁻ salt of succinimidyl ester of RuBDc was from Fluka (Buchs, Switzerland). Trypticase soy broth (TSB) and agar (TSA) media were obtained from Becton, Dickinson and Company (Franklin Lakes, USA). Sepharose CL-4B and Sephadex-G25M columns were from Pharmacia Biotech (Uppsala, Sweden). Centricon YM-100 concentrators were procured from Millipore (Billerica, USA). Coomassie plus protein assay reagent was provided by Pierce (Rockford, USA). All other chemicals were of the reagent grade, and water was deionized with a Milli-Q.

*To whom correspondence should be addressed.

E-mail: jsokang@pusan.ac.kr

Received March 11, 2004; Accepted April 12, 2004

Growth and purification of MS2

The growing of *E. coli* cell strain C-3000 and infection with MS2 followed the procedure of Min Jou *et al.* [21], and purification of the virus was carried out by the procedure of Valegård *et al.* [22] although with several modifications. Briefly, *E. coli* C-3000 was grown in TSB medium until a density of 6×10^8 CFU/ml was reached. CaCl_2 was added to a final concentration of 5 mM, and the cells were infected with phage MS2 at a multiplicity of 5-10 and incubated for another 4 h. Lysis was completed by addition of lysozyme (5 mg/l) and CHCl_3 (5% v/v) in the presence of EDTA (1 mM) and DNase I (1 $\mu\text{g/l}$). Cell debris was pelleted at 8,000 g for 10 min, at 4°C, and discarded. The bacteriophages were separated by ultracentrifugation at 110,000 g for 5 h. The last step of the purification was a gel filtration chromatographic run on a Sepharose CL-4B column. The column was equilibrated and eluted with buffer A (100 mM NaCl, 0.1 mM MgSO_4 , 0.01 mM EDTA, 0.02% sodium azide and 10 mM Tris·HCl, pH 7.4). The purity of the MS2 was analyzed by SDS/polyacrylamide gel electrophoresis.

Labeling of MS2 with $[\text{Ru}(\text{bpy})_2(\text{dcbpy})]^{2+}$

MS2 was labeled with the succinimidyl ester of RuBDC by adding a three-fold molar excess of Ru-NHS in N,N-dimethylformamide to 1 ml of slowly stirred MS2 suspension in 0.05 M carbonate buffer (pH 9.2) followed by an incubation for an hour at room temperature. Centricon YM-100 concentrators were used to change buffer A into 0.05 M carbonate buffer. The resulting labeled MS2 was separated from the free dye by passing the solution through a Sephadex G-25 M column, using buffer A, pH 7.4. The dye/virus protein molar ratio of the Ru-MS2 conjugates was determined by measuring the absorbance of the Ru-MS2 conjugates at 467 nm ($\epsilon_{467 \text{ nm}} = 12,000 \text{ M}^{-1}\text{cm}^{-1}$) and by separately determining the protein concentration with Coomassie plus protein assay reagent. Bovine serum albumin was utilized as a protein standard. The dye/virus protein molar ratio of Ru-MS2 conjugate was 0.63. Because the mature virion contains 180 copies of the coat protein and a single copy of the maturation or A protein, the MW of virus protein was assumed to be that of the coat protein (approximately 14,000). We performed our measurements immediately after labeling.

Absorption and steady-state fluorescence measurements

UV-visible absorption spectra were measured with a Hewlett-Packard 8453 diode array spectrophotometer. Steady-state intensity measurements were carried out using a Cary Eclipse fluorescence spectrophotometer (Varian Inc., Palo Alto, USA). The excitation was at 480 nm while emission was observed at 650 nm.

FD intensity and anisotropy decay measurements

Measurements were performed with an ISS Koala instrument (ISS Inc., Champaign, USA) using a blue LED LNG992CFBW (Panasonic, Japan) as the excitation source. An LED driver LDX-3412 (ILX Lightwave, Boseman, USA) provided 30 mA of current at frequencies from 1 to 9.3 MHz. A 480 ± 20 nm interference

filter and a 630 nm cut-off filter were used for isolating excitation and emission, respectively. Rhodamine B in water ($\tau = 1.68$ ns) was utilized as a lifetime standard. All measurements were performed at 25°C.

The intensity decays were recovered from the FD data in terms of a multiexponential model:

$$I(t) = \sum_{i=1}^n \alpha_i e^{-t/\tau_i} \quad (1)$$

where the preexponential factor α_i is the amplitude of each component, $\sum \alpha_i = 1.0$, τ_i is the decay time, and n is the number of exponential components. These values were determined by a nonlinear least squares analysis as described previously [23, 24]. Mean lifetimes were calculated by:

$$\langle \tau \rangle = \frac{\sum_i \alpha_i \tau_i^2}{\sum_i \alpha_i \tau_i} = \sum_i f_i \tau_i \quad (2)$$

where f_i is the fractional steady-state contribution of each component to the total emission, and $\sum f_i$ is normalized to unity. f_i is given by:

$$f_i = \frac{\alpha_i \tau_i}{\sum_j \alpha_j \tau_j} \quad (3)$$

The best fits were obtained by minimizing χ_R^2 values:

$$\chi_R^2 = \frac{1}{\nu} \sum_{\omega} \left[\left(\frac{\varphi_{\omega} - \varphi_{c\omega}}{\delta\varphi} \right)^2 + \left(\frac{m_{\omega} - m_{c\omega}}{\delta m} \right)^2 \right] \quad (4)$$

where ν is the number of degrees of freedom, and φ_{ω} and m_{ω} are the experimental phase and modulation, respectively. The subscript c is used to indicate calculated values for assumed values of α_i and τ_i , and $\delta\varphi$ and δm are the experimental uncertainties.

The FD anisotropy decays were also analyzed in terms of the multiexponential model:

$$r(t) = \sum_i r_0 g_i e^{-t/\theta_i} \quad (5)$$

where g_i is the amplitude of the anisotropy component with a rotational correlation time θ_i , $\sum g_i = 1.0$, and r_0 is the anisotropy in the absence of rotational diffusion. The total anisotropy r_0 was a fitted parameter. The modulated anisotropy r_{ω} was calculated by:

$$r_{\omega} = \frac{\Lambda_{\omega} - 1}{\Lambda_{\omega} + 2} \quad (6)$$

where Λ_{ω} is the ratio of the amplitudes of the parallel and the perpendicular components of the modulated emission.

RESULTS AND DISCUSSION

Fig. 1 shows the chemical structure of the succinimidyl ester of RuBDC. The absorption and emission spectra of RuBDC conjugated to MS2 are shown in Fig. 2. These spectra are normalized to unity to facilitate comparison. As can be seen in Fig. 2, RuBDC displays both long-wavelength absorption and emission maxima and the large Stokes' shift, with the emission shifting over 180 nm from the absorption maximum. The long-wavelength absorption allowed us to use a simple and inexpensive blue LED as the light source. The long-wavelength emission is valuable because sample autofluorescence is minimized at longer wavelengths.

To determine whether RuBDC can yield useful information about macromolecular dynamics, we performed FD intensity and anisotropy decay measurements of RuBDC-labeled MS2. The FD intensity decays of RuBDC conjugated to MS2 are shown in Fig. 3. The frequency responses are centered near 0.5-0.6 MHz, and the optimal output of an LED is easily modulated at kilohertz to low megahertz frequencies. The intensity decays were analyzed in terms of the multiexponential model according to Eqs. (1) - (4), and the result is

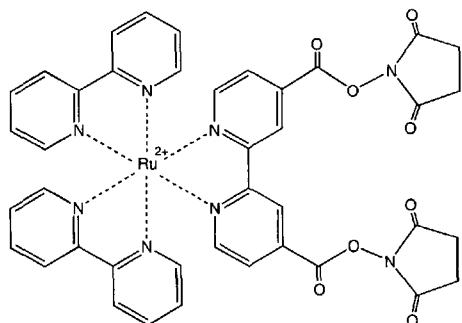


Fig. 1. Chemical structure of succinimidyl ester of $[\text{Ru}(\text{bpy})_2(\text{dcbpy})]^{2+}$.

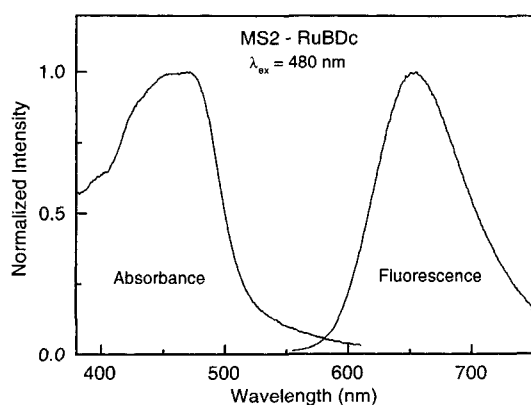


Fig. 2. Absorption and emission spectra of $[\text{Ru}(\text{bpy})_2(\text{dcbpy})]^{2+}$ conjugated to RNA bacteriophage MS2.

summarized in Table 1. The intensity decays were best fit by a sum of two exponentials, and the mean intensity decay time was 442.2 ns.

In addition to the intensity decay measurements, the FD anisotropy decays of RuBDC conjugated to MS2 were also measured (Fig. 4). Bacteriophage MS2 has overall icosahedral symmetry. The virus has a spherical shape with a diameter of 250-260 Å [25, 26]. As expected for a spherical molecule [27], the anisotropy decay data were best fit using the single exponential model, and the result is summarized in Table 2. The rotational correlation time (θ) was 2334.9 ns and appears to be consistent with that expected for overall rotational diffusion of MS2. The measured θ value was compared with the values predicted for anhydrous virus and for a hydrous sphere (Table 3). The molecular volume (V) of the anhydrous virus can be calculated from its MW and partial specific volume (\bar{v}) using $V = (\text{MW} \times \bar{v})/N$ where N is the Avogadro's

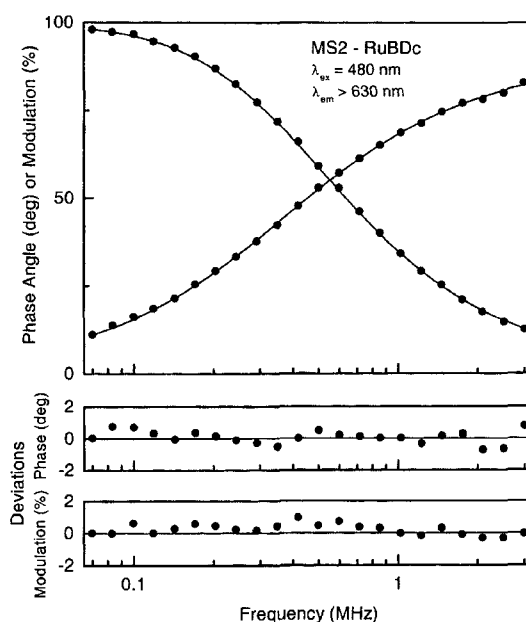


Fig. 3. Frequency-domain intensity decays of $[\text{Ru}(\text{bpy})_2(\text{dcbpy})]^{2+}$ conjugated to RNA bacteriophage MS2. The symbols in the first panel represent the measured phase and modulation values. The solid lines show the best multiexponential fits to the data. The middle and lower panels show plots of the residuals between the experimental data and the fitted curve.

Table 1. Multiexponential intensity decay analysis of $[\text{Ru}(\text{bpy})_2(\text{dcbpy})]^{2+}$ conjugated to RNA bacteriophage MS2

τ_i (ns)	α_i	f_i^a	$\langle \tau \rangle^a$ (ns)	χ_R^2 (b)
265.6	0.32	0.20	442.2	2.6
486.8	0.68	0.80		

^aFractional intensities f_i and mean lifetimes $\langle \tau \rangle$ were calculated using Eqs. (3) and (2), respectively.

^bThe χ_R^2 values were calculated by Eq. (4), and the standard errors of phase angle and modulation were set at 0.2° and 0.005, respectively.

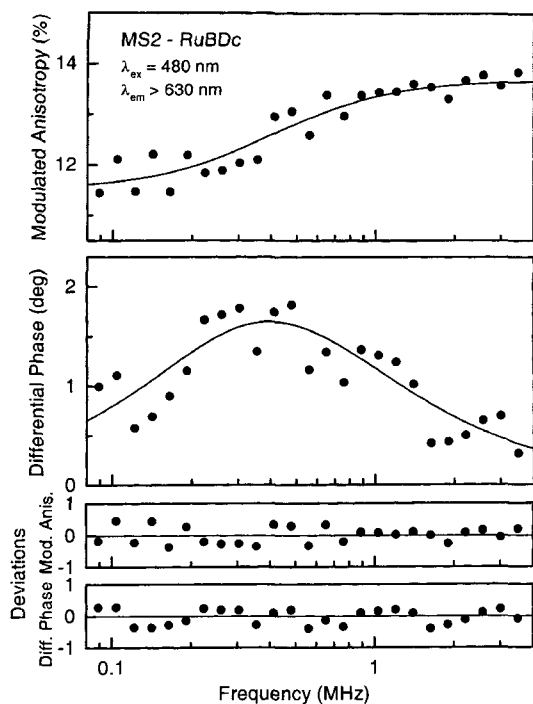


Fig. 4. Anisotropy decays of $[\text{Ru}(\text{bpy})_2(\text{dcbpy})]^{2+}$ conjugated to RNA bacteriophage MS2. The symbols in the first and second panels represent the calculated modulated anisotropy and the measured phase shift values, respectively. The solid lines show the best single exponential fits to the data. The lower two panels show plots of the residuals between the experimental data and the fitted curve.

Table 2. Multiexponential anisotropy decay analysis of $[\text{Ru}(\text{bpy})_2(\text{dcbpy})]^{2+}$ conjugated to RNA bacteriophage MS2

θ_i	$r_0^*g(i)$	$\Sigma(r_0^*g(i))$	χ_R^2 ^{a)}
2334.9	0.137	0.137	2.9

^{a)}The χ_R^2 values were calculated by Eq. (4), and the standard errors of phase angle and modulation were set at 0.2° and 0.005, respectively.

constant. We also calculated the volume of a hydrous sphere from the diameter data of MS2 in the literatures [25, 26]. Using these values and the Perrin equation, we calculated the expected rotational correlation times (Table 3). The observed correlation time is larger than the calculated values. It is about

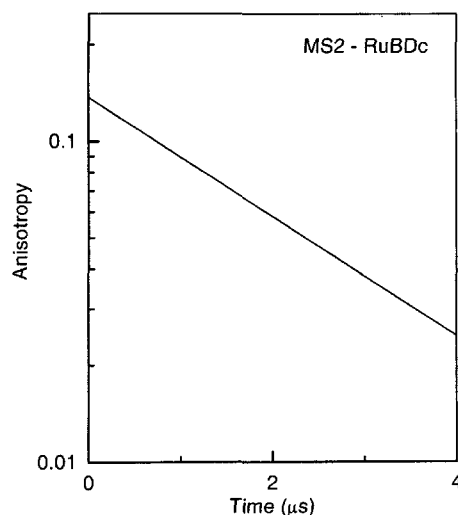


Fig. 5. Time-domain representation of anisotropy decays of $[\text{Ru}(\text{bpy})_2(\text{dcbpy})]^{2+}$ conjugated to RNA bacteriophage MS2.

2.4 times larger than the value for anhydrous virus and still larger than the value for a hydrous sphere. Fig. 4 (top panel) also shows the modulated anisotropy values for RuBDC conjugated to MS2. At low frequency, the modulated anisotropy r_ω is equal to the steady-state anisotropy. The value of r_ω at low frequency was much larger than that of IgM which has a MW of 9×10^5 [12]. It is informative to examine the anisotropy decays in the time-domain reconstructed from the FD data (Fig. 5). The time-domain representation clearly shows the single exponential anisotropy decay, which is typical for a spherical molecule.

In the present study, we demonstrated the usefulness of RuBDC, a long-lifetime MLC, for probing macromolecular hydrodynamics. The use of RuBDC enabled us to measure the rotational correlation time up to several microseconds. However, it should be pointed out that it was not possible to accurately measure the overall rotational correlation time of MS2 which has a MW of 3.9×10^6 [20]. Information on the rotational motion is usually available over a time scale not exceeding three times the lifetime of the fluorophore, after which there is too little signal for accurate anisotropy measurement. In addition, the lifetime of RuBDC is too short

Table 3. Molecular volumes (V) and calculated rotational correlation times (θ) of RNA bacteriophage MS2^{a)}

MW	Anhydrous Virus			Hydrous Sphere		
	\bar{v}	V^b (nm ³)	θ (ns)	r (Å)	V^c (nm ³)	θ (ns)
3.9×10^6 [20]	0.703 [25]	4553	985	125 [25] –	8181 –	1770 –
				130 [26]	9203	1991

^{a)}MW = molecular weight; \bar{v} = partial specific volume; V = molecular volume; θ = rotational correlation time; and r = radius. The rotational correlation times (θ) were calculated according to the Perrin equation $\theta = \eta V / RT$, where η is the viscosity, V is the molecular volume, R is the gas constant, and T is the absolute temperature. The numbers in brackets refer to those of references.

^{b)}Calculated from MW and \bar{v} using $V = (\text{MW} \times \bar{v}) / N$ where N is the Avogadro's constant.

^{c)}Calculated from r .

to measure the overall rotational correlation times of larger viruses than MS2.

Rotational motions of biological macromolecules have occasionally been measured using phosphorescence. However, MLCs have several advantages over the phosphorescent probes. In contrast to phosphorescence, the fluorescence from MLCs can be measured in the presence of dissolved oxygen, whereas phosphorescence is usually completely quenched. Additionally, there are relatively few phosphorescent probes, but there are numerous MLCs. The use of long-lifetime MLCs to measure dynamics of biological macromolecules is just beginning, and additional MLCs with longer lifetimes, polarized emission, and higher quantum yields are yet to be developed.

An important point of the present study is our use of a semiconductor light source for the FD intensity and anisotropy decay measurements. A variety of LEDs including the high intensity UV, blue and green LEDs have been developed as an inexpensive and convenient light source. LEDs are easily modulated up to hundreds of MHz without the need for a Pockels cell [28]. We believe that LEDs will become an ideal light source for measuring microsecond dynamics of biological macromolecules.

Acknowledgments - This research was supported by Pusan National University Research Grant. JSK deeply thanks Professor Govind Rao, Dept. of Chemical and Biochemical Engineering, The University of Maryland, Baltimore County, Baltimore, USA for providing instrumentation.

REFERENCES

- DeGraff, B. A. and Demas, J. N. (1994) Direct measurement of rotational correlation times of luminescent ruthenium(II) molecular probes by differential polarized phase fluorometry. *J. Phys. Chem.* **98**, 12478-12480.
- Lakowicz, J. R., Gryczinski, I., Piszczek, G., Tolosa, L., Nair, R., Johnson, M. L. and Nowaczyk, K. (2000) Microsecond dynamics of biological molecules. *Methods Enzymol.* **323**, 473-509.
- Terpetschnig, E., Szmecinski, H. and Lakowicz, J. R. (1997) Long-lifetime metal-ligand complexes as probes in biophysics and clinical chemistry. *Methods Enzymol.* **278**, 295-321.
- Haugen, G. R. and Lytle, F. E. (1981) Quantitation of fluorophores in solution by pulsed laser excitation of time-filtered detection. *Anal. Chem.* **53**, 1554-1559.
- Castellano, F. N., Dattelbaum, J. D. and Lakowicz, J. R. (1998) Long-lifetime Ru(II) complexes as labeling reagents for sulfhydryl groups. *Anal. Biochem.* **255**, 165-170.
- Guo, X. -Q., Castellano, F. N., Li, L., Szmecinski, H., Lakowicz, J. R. and Sipior, J. (1997) A long-lived, highly luminescent Re(I) metal-ligand complex as a biomolecular probe. *Anal. Biochem.* **254**, 179-186.
- Murtaza, Z., Herman, P. and Lakowicz, J. R. (1999) Synthesis and spectral characterization of a long-lifetime osmium(II) metal-ligand complex: a conjugatable red dye for applications in biophysics. *Biophys. Chem.* **80**, 143-151.
- Szmecinski, H., Terpetschnig, E. and Lakowicz, J. R. (1996) Synthesis and evaluation of Ru-complexes as anisotropy probes for protein hydrodynamics and immunoassays of high-molecular-weight antigens. *Biophys. Chem.* **62**, 109-120.
- Szmecinski, H., Castellano, F. N., Terpetschnig, E., Dattelbaum, J. D., Lakowicz, J. R. and Meyer, G. J. (1998) Long-lifetime Ru(II) complexes for the measurement of high molecular weight protein hydrodynamics. *Biochim. Biophys. Acta* **1383**, 151-159.
- Terpetschnig, E., Szmecinski, H., Malak, H. and Lakowicz, J. R. (1995) Metal-ligand complexes as a new class of long-lived fluorophores for protein hydrodynamics. *Biophys. J.* **68**, 342-350.
- Terpetschnig, E., Dattelbaum, J. D., Szmecinski, H. and Lakowicz, J. R. (1997) Synthesis and spectral characterization of a thiol-reactive long-lifetime Ru(II) complex. *Anal. Biochem.* **251**, 241-245.
- Kang, J. S., Piszczek, G. and Lakowicz, J. R. (2002) High-molecular-weight protein hydrodynamics studied with a long-lifetime metal-ligand complex. *Biochim. Biophys. Acta* **1597**, 221-228.
- Guo, X. -Q., Castellano, F. N., Li, L. and Lakowicz, J. R. (1998) A long-lifetime Ru(II) metal-ligand complex as a membrane probe. *Biophys. Chem.* **71**, 51-62.
- Li, L., Szmecinski, H. and Lakowicz, J. R. (1997) Synthesis and luminescence spectral characterization of long-lifetime lipid metal-ligand probes. *Anal. Biochem.* **244**, 80-85.
- Li, L., Castellano, F. N., Gryczinski, I. and Lakowicz, J. R. (1999) Long-lifetime lipid rhenium metal-ligand complex for probing membrane dynamics on the microsecond timescale. *Chem. Phys. Lipids* **99**, 1-9.
- Lakowicz, J. R., Malak, H., Gryczinski, I., Castellano, F. N. and Meyer, G. J. (1995) DNA dynamics observed with long lifetime metal-ligand complexes. *Biospectroscopy* **1**, 163-168.
- Malak, H., Gryczinski, I., Lakowicz, J. R., Meyers, G. J. and Castellano, F. N. (1997) Long-lifetime metal-ligand complexes as luminescent probes for DNA. *J. Fluorescence* **7**, 107-112.
- Kang, J. S., Abugo, O. O. and Lakowicz, J. R. (2002) Dynamics of supercoiled and linear pTZ18U plasmids observed with a long-lifetime metal-ligand complex. *Biopolymers* **67**, 121-128.
- Kang, J. S., Abugo, O. O. and Lakowicz, J. R. (2002) Dynamics of supercoiled and relaxed pTZ18U plasmids probed with a long-lifetime metal-ligand complex. *J. Biochem. Mol. Biol.* **35**, 389-394.
- Camerini-Otero, R. D., Franklin, R. M. and Day, L. A. (1974) Molecular weights, dispersion of refractive index increments, and dimensions from transmittance spectrophotometry. Bacteriophages R17, T7, and PM2, and tobacco mosaic virus. *Biochemistry* **13**, 3763-3773.
- Min Jou, W., Raeymaekers, A. and Fiers, W. (1979) Crystallization of bacteriophage MS2. *Eur. J. Biochem.* **102**, 589-594.
- Valegård, K., Unge, T., Montelius, I. and Strandberg, B. (1986) Purification, crystallization and preliminary X-ray

- data of the bacteriophage MS2. *J. Mol. Biol.* **190**, 587-591.
23. Lakowicz, J. R., Laczko, G., Cherek, H., Gratton, E. and Limkeman, M. (1984) Analysis of fluorescence decay kinetics from variable-frequency phase-shift and modulation data. *Biophys. J.* **46**, 463-477.
 24. Gratton, E., Limkeman, M., Lakowicz, J. R., Maliwal, B. P., Cherek, H. and Laczko, G. (1984) Resolution of mixtures of fluorophores using variable-frequency phase and modulation data. *Biophys. J.* **46**, 479-486.
 25. Boedtker, H. and Gesteland R. F. (1975) Physical properties of RNA bacteriophages and their RNA. *In: RNA Phages*. Ed. by Zinder, N. D. Cold Spring Harbor Laboratory, New York, pp. 1-28.
 26. Strauss, J. H. Jr. and Sinsheimer, R. L. (1963) Purification and properties of bacteriophage MS2 and of its nucleic acid. *J. Mol. Biol.* **7**, 43-54.
 27. Lakowicz, J. R. (1999) *Principles of Fluorescence Spectroscopy*, 2nd Ed., Kluwer Academic/Plenum Publishers, New York, pp. 304.
 28. Sipior, J., Carter, J. M., Lakowicz, J. R. and Rao, G. (1996) Single quantum well light-emitting diodes demonstrated as excitation sources for nanosecond phase modulation fluorescence lifetime measurements. *Rev. Sci. Instr.* **67**, 3795-3798.